

HYDROTHERMAL GROWTH OF $Zn_5(OH)_6(CO_3)_2$ AND ITS THERMAL TRANSFORMATION INTO POROUS ZnO FILM USED FOR DYE-SENSITIZED SOLAR CELLS

HIDROTHERMALNA RAST $Zn_5(OH)_6(CO_3)_2$ S TERMIČNO TRANSFORMACIJO V POROZNO PLAST ZnO, UPORABLJENO ZA ELEKTROKEMIJSKE SONČNE CELICE

Marko Bitenc^{1,2}, Zorica Crnjak Orel^{1,2}

¹National Institute of Chemistry, Hajdrihova 19, SI-1000, Ljubljana, Slovenia

²Center of Excellence for Polymer Materials and Technologies, Tehnološki park 24, 1000 Ljubljana, Slovenia
marko.bitenc@ki.si, zorica.crnjak.orel@ki.si

Prejem rokopisa – received: 2011-02-14; sprejem za objavo – accepted for publication: 2011-03-15

Zinc oxide (ZnO) films, composed of nano-sheets, were prepared by the thermal decomposition of hydrozincite film precursor ($Zn_5(OH)_6(CO_3)_2$, ZnHC). The ZnO film kept the morphology on the microscale level during the heat treatment, while the thermal decomposition caused the formation of a nano-porous structure of the nano-sheets' surface. ZnHC precursor was hydrothermally synthesized on the conductive glass from zinc nitrate and urea. The influence of media (water or mixture of water/ethylene glycol), PVP-K additive and the concentration of the initial reagents, on the morphology of the film were observed. The growth and morphology of the ZnHC film was followed with FE-SEM microscopy and the formation mechanism of the ZnHC film, formed in the water, was proposed. The assumed growth mechanism follows the concept of a self-assembling mechanism of the nanometer-sized building units into nano-sheets of ZnHC with a thickness of ≈ 20 nm. These nano-sheets are further agglomerating into porous film. The thickness of the film was around (5, 8, 10 and 20) μm after (2, 3, 4 and 24) h of synthesis, respectively. The addition of PVP-K and ethylene glycol retards the growth of ZnHC film. Moreover, the addition of PVP-K affects the interactions between particles and the substrate, which enable the parallel growth of the nano-sheets on the substrate surface. As prepared ZnO films were used for DSSCs, where the conversion efficiency was ≈ 0.6 %.

Keywords: ZnO, hydrozincite, hydrothermal, precipitation, particles growth, SEM, DSSCs

Cinkov oksid (ZnO) smo pripravili kot tako plast na prevodni podlagi s termično obdelavo prekursorja hidrocinkita ($Zn_5(OH)_6(CO_3)_2$, ZnHC). Tako pripravljena plast je bila sestavljena iz nanolističev, ki so po termični obdelavi obdržali svojo obliko na mikroskopskem nivoju, medtem ko so na njihovi površini nastale luknjice nanovelikosti. Plast ZnHC smo pripravili s hidrotermalno precipitacijo cinkovega nitrata s sečnino. Ob tem smo opazovali vpliv različnih koncentracij začetnih reagentov, medija (voda in mešanica vode/etilen glikola) in dodatkov (PVP-K) na rast in morfologijo nastalega produkta, ki smo ju spremljali z FE-SEM-mikroskopijo. Na osnovi rezultatov opazovanja vzorcev, pripravljenih v vodnem mediju, smo predpostavili mehanizem rasti plasti ZnHC. Ugotovili smo, da ta mehanizem sledi konceptu povezovanja nanogradnikov v večje urejene kristalne mikrostrukture z obliko nanolističev z debelino ≈ 20 nm. Nanolističi ZnHC se na podlagi aglomerirajo v porozno plast. Debelina plasti je bila približno 5 μm po 2 h, 8 μm po 3 h, 10 μm po 4 h in 20 μm po 24 h sinteze. Dodatek PVP-K in etilen glikol upočasnita rast plasti ZnHC. Poleg tega je dodatek PVP-K vplival na interakcije med lističi in podlago, ki omogočijo rast lističev vzporedno s površino podlage. Plasti ZnO smo uporabili za izdelavo elektrokemijskih sončnih celic, katerih učinkovitost pretvorbe sončne energije v električno je $\approx 0,6$ %.

Ključne besede: ZnO, hidrocinkit, hidrotermalno, precipitacija, rast delcev, SEM, elektrokemijske sončne celice

1 INTRODUCTION

ZnO nano-sheets have attracted increasing interest on account of their specific microstructure and potential applications in many areas, such as chemical sensors, photocatalysts, phosphors and dye-sensitized solar cells (DSSCs).¹⁻⁴ For these applications the ZnO particles are typically prepared as a film on various glass or polymer substrates, covered with transparent conducting oxides (TCO). ZnO films and powders, reported in the literature, are most commonly composed of particles with the hexagonal rod-like morphology^{2,5-9} and rarely with nano-sheet morphology prepared from the corresponding layered ZnHC precursor with the thermal decomposition.^{1,3,10} The hydrothermal precipitation of ZnHC from zinc nitrate with urea was presented in our papers, where the influence of the different additives on the final morphology of the particles was studied in a closed

reactor system.¹¹ The precipitated ZnHC decomposed into ZnO in only one relatively sharp step. The growth mechanism of the ZnHC particles based on the combination of in-situ SAXS measurement and ex-situ electron microscopy was also presented in our recently published paper.⁴

The interest in dye-sensitized solar cells (DSSCs) has increased due to reduced energy sources and higher energy production costs. For the most part, titania (TiO_2) has been the material of choice for dye-sensitized solar cells and so far have shown the highest overall light conversion efficiency ≈ 11 %.¹² However, ZnO has recently been explored as an alternative material in DSSCs with great potential since it has a bandgap similar to TiO_2 at 3.2 eV and has a much higher electron mobility ($\approx (115-155) \text{ cm}^2/(\text{V s})$) than TiO_2 ($\approx 10^{-5} \text{ cm}^2/(\text{V s})$). In addition, ZnO has ability of simpler tailoring of the

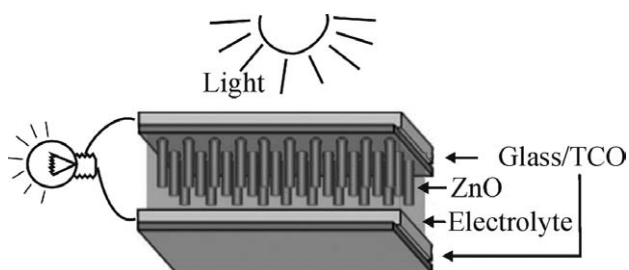


Figure 1: Schematic description of DSSCs applying ZnO nano particles as the electron transport material, dye for light-harvesting and electrolyte with a I^-/I_3^- redox couple

Slika 1: Shema elektrokemijske sončne celice, sestavljene iz ZnO-polprevodnika za transport elektronov, barvila na polprevodniku in elektrolita z redoks parom I^-/I_3^-

particles' morphology. Also it can not be neglected, that the initial compounds for the production of ZnO are much cheaper as compared to TiO_2 . The efficiency of the DSSCs prepared from the ZnO nano-sheet film is lower regarding DSSCs that use TiO_2 for their preparation.^{1,3} In the literature it was reported that DSSCs with the ZnO nano-sheets film electrode, prepared from ZnHC precursor, have the efficiency around 4 %.

Figure 1 shows a schematic representation of DSSCs applying vertically-aligned ZnO nanostructured electrode. The typical basic configuration is as follows: At the heart of the device is the mesoporous oxide layer composed of ZnO film. Typically, the film thickness is $\approx 10 \mu m$ and the porosity is 50–60 %. The mesoporous layer of ZnO is deposited on substrate (polymer or glass) coated with TCO, such as indium tin oxide (ITO) fluorine doped tin oxide (FTO) or aluminium doped zinc oxide (AZO). Attached to the surface of the ZnO film is a monolayer of the charge-transfer dye, mostly based on ruthenium. Photoexcitation of the later results in the injection of an electron into the conduction band of the oxide, leaving the dye in its oxidized state. The dye is restored to its ground state by electron transfer from the electrolyte, which is usually an organic solvent containing the iodide/triiodide redox system. The regeneration of the sensitizer by iodide intercepts the recapture of the conduction band electron by the oxidized dye. The I_3^- ions formed by oxidation of I^- diffuse because of a short distance ($< 50 \mu m$) through the electrolyte to the cathode, which is coated with a thin layer of platinum catalyst, where the regenerative cycle is completed by electron transfer to reduce I_3^- to I^- .

In this work we present the preparation of ZnHC film from zinc nitrate and urea in different media, such as water, water/EG mixture and in water with addition of PVP-K. The growth of the ZnHC film, which was later thermally decomposed into ZnO, was followed with FE-SEM microscopy. The formation mechanism of the ZnHC film, in water, is presented. As prepared ZnO films were used for DSSCs preparation.

2 EXPERIMENTAL

All reagents in the experimental work were of analytical reagent grade. To avoid hydrolysis upon storage, fresh stock solutions prepared from $Zn(NO_3)_2 \times 6H_2O$ (Aldrich) and urea (Aldrich) in millique water were used. The detailed experimental conditions for the preparation of samples are given in **Table 1**. The initial concentrations of Zn^{2+} ions were 0.1 M and 0.01 M and urea 0.5 M and 0.05 M. The concentration of urea was five times higher than Zn^{2+} in all experiments. As solvents water and a mixture of water and ethylene glycol (EG, Merck) with the volume ration 1 : 1, were used. Experiments were performed without and in the presence of PVP-K additive. The additive was dissolved in the initial reactive mixture before hydrolysis took place. The concentration of additive was 10 mg/mL throughout the experimental study.

Table 1: Experimental conditions for the sample preparations in water and water/ethylene glycol (EG) mixture, with and without additive

Tabela 1: Pregled eksperimentov za pripravo tanke plasti na prevodnem steklu v vodi in mešanici voda/etilen glikol (EG) brez dodatka in z njim

Sample	Medium	Solution mL	C (Zn^{2+}) M	PVP-K mg/mL	Time h
A	water	50	0.1	/	2, 3, 4, 24
B	water	50	0.01	10	24
C	water + EG	25 + 25	0.01	/	72

The experiments were carried out in laboratory bottles, where the total volume of reaction mixture was 50 mL. Borosilicate glass slides, with one side covered with the $SnO_2 : F$, were used as substrates for the film deposition. The substrates were placed into laboratory bottles filled with Zn/urea solution, sealed and kept at 90 °C for 2 h to 72 h in drying oven (Kambič, Easy) as presented in **Figure 2a**. During these experiments, the temperature was measured in the center of laboratory bottle with Pt100. The resulting temperature profile shows that maximum temperature was reached after around 100 min and was constant (85 °C) during the synthesis (**Figure 2b**). After the deposition, the obtained

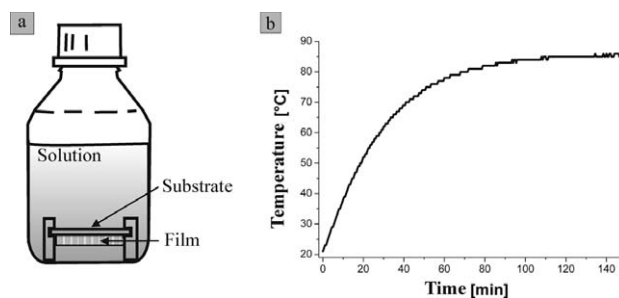


Figure 2: a – Schematic description of the film preparation. b – Temperature profile in laboratory bottle

Slika 2: a – Shema priprave delcev na podlagi; b – Temperaturni profil v laboratorijski steklenici

hydrozincite films were rinsed with ethanol and dried at room temperature. The films were thermally treated at 300 °C for 30 min in air. As prepared ZnO film were used for DSSCs preparation.

The DSSCs were prepared and characterized in Laboratory of Photovoltaics and Optoelectronics of the Faculty of Electrical Engineering (University of Ljubljana) as previously reported in their papers.^{13–15}

Samples were characterized by scanning field emission electron microscopy (FE-SEM, Zeiss Supra 35 VP). IR-spectra were obtained on an FTIR spectrometer (Perkin Elmer 2000) in the spectral range between 4000 cm^{-1} and 400 cm^{-1} with a spectral resolution of 2 cm^{-1} . The KBr pellet technique was used for the sample preparation.

3 RESULTS AND DISCUSSION

The FE-SEM microstructure of the hydrozincite (ZnHC) film marked as Samples A, which was prepared on the glass substrate coated with $SnO_2 : F$ in water medium after (2, 3, 4 and 24) h are presented in **Figure 3** (top-view) and **Figure 4** (cross-section). The porous spherical structures composed of nano-sheets with thickness around 20 nm was observed after 2 h of synthesis as presented in **Figures 3a and 4a**. The thickness of ZnHC film is round 5 μm after 2 h of the synthesis as presented in **Figure 4a**. From the particles' microstructure and morphology, we could propose that

ZnHC nano sheets begin to grow from one point (initial nucleus) on a substrate and not separately, which is typical for the growth of the pure hexagonal ZnO.^{16–18} The top-view and the cross-sectional micrographs of the substrate's microstructure of the Sample A, obtained after 3 h (**Figures 3b and 4b**) and 4 h (**Figures 3c and 4c**) are presented, respectively. The nano-sheets cover the entire surface of the substrate. The thickness of ZnHC film is about 8 μm after 3 h and about 10 μm after 4 h of the synthesis. The thickness of the film increases up to 20 μm after 24 h of synthesis (**Figure 4d**). We found that nano-sheets grow in the length and width, while the thickness of the nano-sheets was remaining constant about 20 nm (**Figure 3d**). The ZnHC film was found on substrate only on the conductive side and when this side was facing down (**Figure 2a**). Scratches and dirt on conductive side of the substrate retard and limited the growth of the particles.

The proposed growth mechanism of the ZnHC film on the TCO substrate is schematically presented in **Figure 5**. We propose that growth of the nano-sheets follows the growth mechanism of the ZnHC particles which was recently presented by our group. We explain the growth mechanism by the "non-classical crystallization" concept of a self-assembling mechanism. The growth mechanism predicts the rapid formation of nanometer-sized building units. The size of these nano building units, stable only in the reaction medium, remains nearly constant during the synthesis, as the concentration of the nano building units increases

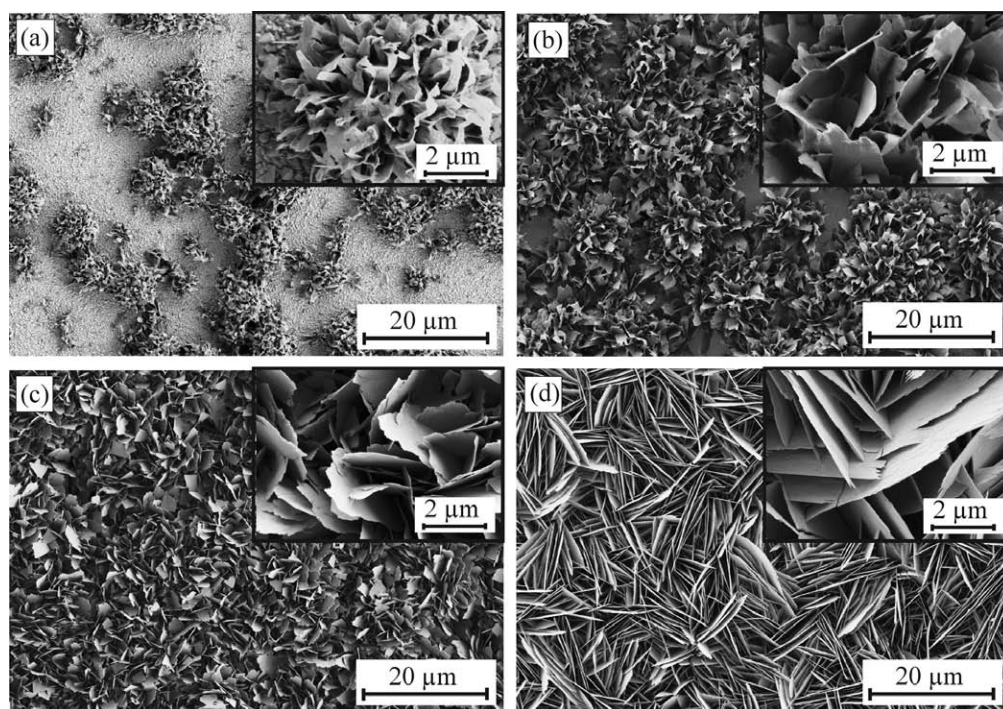


Figure 3: FE-SEM microstructure of the ZnHC of Sample A prepared on the glass substrate in water medium after (a) – 2 h, (b) – 3 h, (c) – 4 h in (d) – 24 h

Slika 3: FE-SEM-mikrostruktura ZnHC-vzorca A, pripravljenega na prevodnem steklu v vodnem mediju pri različnih časih: (a) – 2 h, (b) – 3 h, (c) – 4 h in (d) – 24 h

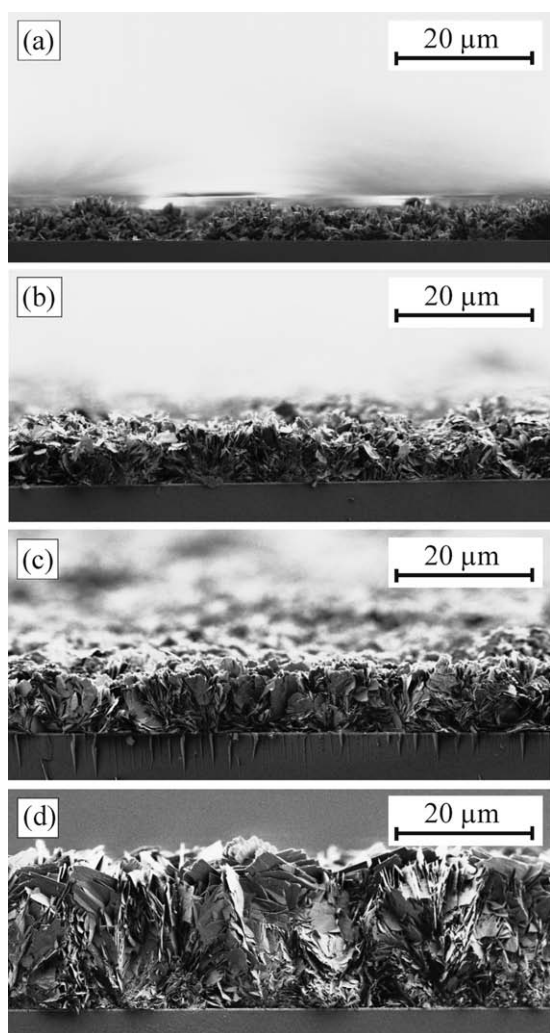


Figure 4: FE-SEM microstructure of the ZnHC film cross-section of Sample A prepared on glass substrate in water medium after (a) – 2 h, (b) – 3 h, (c) – 4 h in (d) – 24 h

Slika 4: FE-SEM-mikrostruktura prereza plasti ZnHC-vzorca A, pripravljenega na steklu v vodnem mediju ob različnih časih: (a) – 2 h, (b) – 3 h, (c) – 4 h in (d) – 24 h

throughout the reaction. These leaves of ZnHC are further agglomerated into porous, nano-sheet like film. The thickness of the film is increasing with time.

The influence of the medium (a mixture of water/EG at volume ratio 1/1), PVP-K additive and the concentration of the initial reagents, on the morphology and growth of the film were observed (**Figure 6**). Microstructure of Sample B, prepared with the addition of PVP-K (10 mg/mL) after 24 h of synthesis, is presented in **Figure 6a**. We found that the addition of PVP-K noticeably retard the growth of ZnHC film, since the microstructure of the particles is similar to the film of Sample A prepared in water after 2 h of the synthesis (**Figure 3a**). Additionally, we observed the parallel (according to substrate surface) formation of nano-sheets in the synthesis with the PVP-K, as it is presented in **Figure 6a**. We assume the addition of PVP-K affects

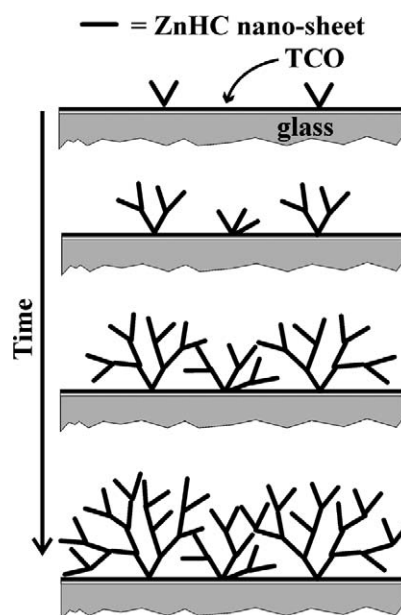


Figure 5: Schematic description of the growth mechanism of ZnHC film on the substrate

Slika 5: Shematično predstavljen mehanizem rasti plasti ZnHC na podlagi

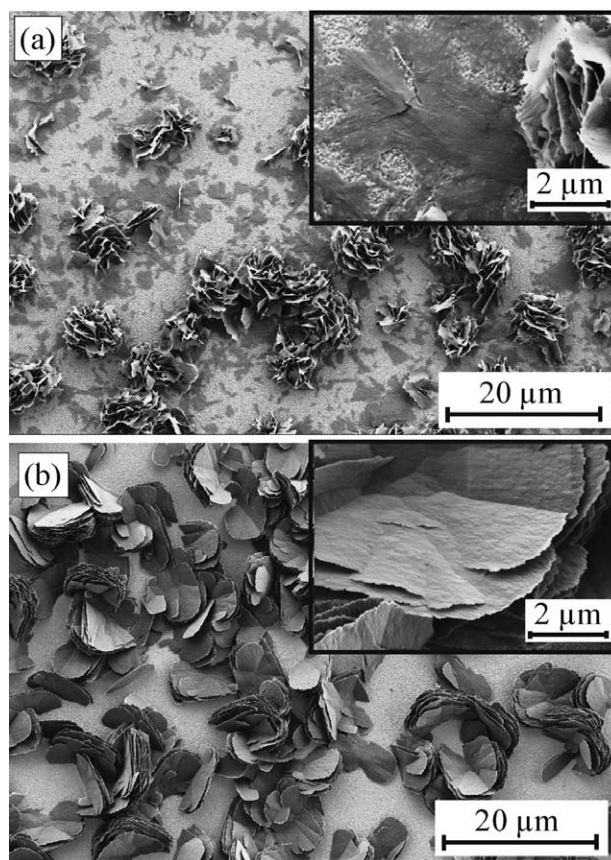


Figure 6: FE-SEM microstructure of the ZnHC samples prepared on glass substrate: (a) – Sample B, prepared in water with PVP-K additive and (b) – Sample C prepared in water/EG mixture

Slika 6: FE-SEM-mikrostruktura delcev ZnHC, pripravljenih na steklu: (a) – vzorec B, pripravljen v vodi z dodatkom PVP-K in (b) – vzorec C, pripravljen v mešanici voda/EG

hydrophilic/hydrophobic interactions between particles and the substrate, which enable the parallel growth of the nano-sheets on the substrate surface.¹ Microstructure of Sample C, prepared in the mixture of water/EG 1/1, after 72 h of synthesis is shown in **Figure 6b**. Particle growth is retarded even at a higher concentration of initial reagents.

As prepared ZnHC films on the TCO substrate were additionally heat-treated for 30 min at 300 °C. The FE-SEM microstructure of heat treated film of Sample A (4 h) is presented in **Figure 7** as an example. Similar effects were observed also in other samples (micrographs not presented in this paper). Generally the size and the morphology of the particles observed by FE-SEM remain practically identical on the micro scale during heat treatment (**Figure 7**). However, the annealing caused the formation of a nanoporous structure on the particles' surface, which revealed an increased specific surface area.¹¹

The samples were characterized by FTIR (**Figure 8**) before and after heat treatment to determine the chemical composition of the prepared films. The FTIR spectrum of Sample A, prepared after 24 h of synthesis and before heat treatment, is presented in **Figure 8a**. The presence of carbonate groups in the ZnHC product was confirmed

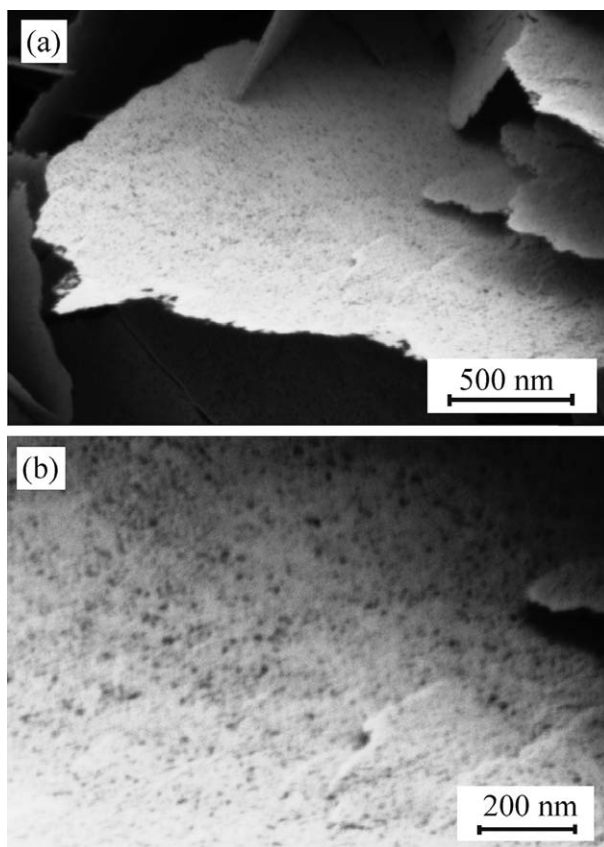


Figure 7: FE-SEM microstructure of ZnO film of Sample A (4 h) after 30 min of heat treatment at 300 °C

Slika 7: FE-SEM-mikrostruktura plasti ZnO-vzorca A (4 h) po 30 min termični obdelavi na 300 °C

by bands in the spectral range from 1600 cm^{-1} and 1200 cm^{-1} , i.e. the frequency at 1507 cm^{-1} and 1390 cm^{-1} , and additionally with the frequency at 1044 cm^{-1} , 956 cm^{-1} and at 708 cm^{-1} .^{4,19} After thermal treatment (300 °C) of this sample (Sample A, 24 h) the band at 421 cm^{-1} with a pronounced shoulder at 530 cm^{-1} in the IR spectra (**Figure 8b**) confirmed the presence of ZnO.

ZnO films, obtained after 4 h and 24 h of the synthesis and additionally heat treated for 30 min at 300 °C, were used for the preparation of DSSCs.^{12–15} Average current density-voltage characteristics of electrochemical solar cells under standard conditions (100 mW/cm^2 , 25 °C) are summarized in **Table 2**. The density-voltage characteristic curve of the best DSSCs, prepared from the ZnO film after 4 h of the synthesis is presented in the **Figure 9**.

Table 2: An average short-circuit photocurrent density (J_{SC}), open-circuit voltage (V_{OC}), fill factor (FF), and conversion efficiency (η) of the DSSCs evaluated under STC (100 mW/cm^2 , 25 °C) for the ZnO films prepared after 4 h and 24 h of synthesis

Tabela 2: Povprečje meritev kratkostične tokovne gostote (J_{SC}), napetosti odprtih sponk (V_{OC}), polnilnega faktorja (FF) in učinkovitost pretvorbe (η) za DSSCs, izmerjen pri standardnih pogojih (100 mW/cm^2 , 25 °C) in z uporabo plasti ZnO pripravljene po 4 h in 24 h sinteze

Synthesis time, h	$J_{SC}/mA/cm^2$	V_{OC}/V	$FF/\%$	$\eta/\%$
4	2.63	0.52	41.93	0.57
24	3.23	0.50	36.37	0.58

An average open-circuit voltage (V_{OC}) 0.52 V and 0.50 V, and conversion efficiency (η) 0.57 % and 0.58 % of the DSSCs, evaluated under STC (100 mW/cm^2 , 25 °C) and prepared from the ZnO films of the 4 h and 24 h synthesis, are comparable. However, the short-circuit photocurrent density (J_{SC}) is higher (3.23 mA/cm^2) in a cell made from the thicker ZnO film ($\approx 20 \mu m$) prepared after 24 h of the synthesis, compared to the J_{SC} of the

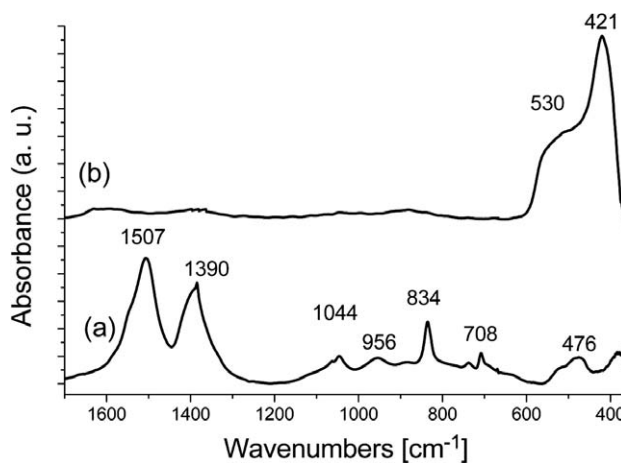


Figure 8: FTIR spectra of Sample A prepared after 4 h of synthesis (a) and with additional heat treatment (b)

Slika 8: FTIR-spekter vzorca A, pripravljenega po 4 h sinteze (a) in po dodatni termični obdelavi (b)

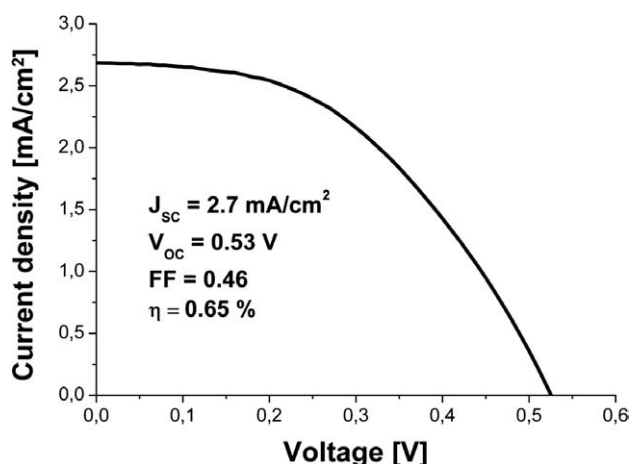


Figure 9: A current density-voltage curve of the dye-sensitized solar cell prepared from ZnO films of Sample A (4 h of synthesis)

Slika 9: Tokovno-napetostni odziv elektrokemijske sončne celice, pripravljen iz plasti ZnO vzorca A (4 h sinteze)

DSSCs prepared from the 10 μm thick ZnO film obtained after 4 h of synthesis. Contrary, the fill factor (FF) 41.93 % is higher in a DSSCs prepared from the thinner ZnO film (4 h synthesis), compared to the FF 36.37 % obtained in the DSSCs with thicker ZnO film. Results prove that larger film thickness increases the amount of adsorbed dyes, which leads to higher J_{SC} . On the other hand, increasing the film thickness decreases FF through diffusion-limited access.¹

The V_{OC} and FF of our DSC cells are comparable to results reported in the literature.^{1,3} On the other hand, the J_{SC} of cells is between 2.63 mA/cm^2 and 3.23 mA/cm^2 in a short circuit, which is almost one third of comparable measurements in literature.^{1,3} The low J_{SC} could be explained by the generation of the Zn^{2+}/dye aggregates. Ru-complexes dyes, such as N-719 (used in our case), are slightly acid, since they could have protons derived from the complex.³ Consequently, the dye-loading solution dissolves the surface of ZnO and makes Zn^{2+}/dye aggregates, which influence on the lower electron injection efficiencies and fill nano-scale pores. The optimization of various parameters including ZnO film fabrication, dyeing time, heating conditions, and so on, will result in the improvement of the conversion efficiency because the FF and V_{OC} in this work are reasonably high.

4 CONCLUSIONS

ZnO film with the nano-sheets porous microstructure was prepared by the thermal decomposition of ZnHC precursor, which was hydrothermally synthesized on the conductive glass from zinc nitrate and urea. The growth mechanism and the morphology of the ZnHC film was followed with SEM microscopy and the formation of the ZnHC film, is proposed by the "non-classical crystalli-

zation" concept of a self-assembling mechanism. The influence of a mixture of water/EG, surfactant additive PVP-K and the concentration of the initial reagents, on the morphology of the film were observed. ZnO films were used for the preparation of DSSCs with the average conversion efficiency around 0.6 %.

ACKNOWLEDGMENT

The authors would like to thank the colleges from Laboratory of Photovoltaics and Optoelectronics (Faculty of Electrical Engineering, UL) for their help regarding DSSC assembling and characterization. We acknowledge the financial support from the Ministry of Higher Education, Science and Technology of the Republic of Slovenia through the contract No. 3211-10-000057 (Center of Excellence for Polymer Materials and Technologies).

5 REFERENCES

- E. Hosono, S. Fujihara, I. Honna, H. S. Zhou, *Adv. Mater.*, 17 (2005) 17, 2091–2094
- I. Gonzalez-Valls, M. Lira-Cantu, *Energy & Environmental Science*, 2 (2009) 1, 19–34
- K. Kakiuchi, M. Saito, S. Fujihara, *Thin Solid Films*, 516 (2008) 8, 2026–2030
- M. Bitenc, P. Podbršček, P. Dubček, S. Bernstorff, G. Dražić, B. Orel, S. Pejovnik, Z. C. Orel, *Chem.–Eur. J.*, 16 (2010) 37, 11481–11488
- Z. Y. Fan, J. G. Lu, *J. Nanosci. Nanotechnol.*, 5 (2005), 10, 1561–1573
- Y. W. Heo, D. P. Norton, L. C. Tien, Y. Kwon, B. S. Kang, F. Ren, S. J. Pearton, J. R. LaRoche, *Materials Science & Engineering R-Reports*, 47 (2004) 1–2, 1–47
- M. Bitenc, P. Podbršček, Z. C. Orel, M. A. Cleveland, J. A. Paramo, R. M. Peters, Y. M. Strzhemechny, *Cryst. Growth Des.*, 9 (2009) 2, 997–1001
- M. Bitenc, G. Dražić, Z. C. Orel, *Cryst. Growth Des.*, 10 (2010) 2, 830–837
- G. Ambrožič, S. D. Škapin, M. Žigon, Z. C. Orel, *J. Colloid Interface Sci.*, 346 (2010) 2, 317–323
- P. Podbršček, Z. C. Orel, J. Maček, *Mater. Res. Bull.*, 44 (2009) 8, 1642–1646
- M. Bitenc, M. Marinšek, Z. C. Orel, *J. Eur. Ceram. Soc.*, 28 (2008) 15, 2915–2921
- T. P. Chou, Q. F. Zhang, G. E. Fryxell, G. Z. Cao, *Adv. Mater.*, 19 (2007) 18, 2588–2595
- M. Hočevar, M. Berginc, M. Topič, U. O. Krašovec, *J. Sol-Gel Sci. Technol.*, 53 (2010) 3, 647–654
- M. Berginc, U. O. Krašovec, M. Hočevar, M. Topič, *Thin Solid Films*, 516 (2008) 20, 7155–7159
- U. O. Krašovec, M. Berginc, M. Hočevar, M. Topič, *Sol. Energy Mater. Sol. Cells*, 93 (2009) 3, 379–381
- A. B. Djurisić, Y. H. Leung, *Small*, 2 (2006) 8–9, 944–961
- L. Schmidt-Mende, J. L. MacManus-Driscoll, *Materials Today*, 10 (2007) 5, 40–48
- A. S. Barnard, Y. Xiao, Z. Cai, *Chem. Phys. Lett.*, 419 (2006), 4–6, 313–316
- M. Bitenc, Z. C. Orel, *Mater. Res. Bull.*, 44 (2009) 2, 381–387